Available online at www.sciencedirect.com
SCIENCE DIRECT®
Journal of Sound and Vibration 280 (2005) 965–981
JOURNAL OF SOUND AND VIBRATION
www.elsevier.com/locate/yjsvi

Signal frequency-based semi-active fuzzy control for two-stage vibration isolation system

Tao Sun*, Zhenyu Huang, Dayue Chen

Department of Information Measurement Technology and Instruments, Shanghai Jiaotong University, Shanghai, 200030, PR China

Received 7 November 2002; accepted 23 December 2003
Available online 23 September 2004

Abstract

In this paper, a novel feed forward control scheme with a fuzzy controller, based on the identification of the signal's main frequency, is proposed to control a semi-active two-stage vibration isolation system such as the floating raft isolation system, whose excitation signal changes regularly. A fuzzy controller is employed in this method to achieve the best isolation effect by analyzing the main frequency's characteristics of the excitation signal, such as amplitude and position, and a bypass electro-rheological (ER) damper is applied to achieve the best control effect more rapidly and accurately. The inputs of the fuzzy controller are the characters of the signal's main frequency and the output is the effect coefficient of the main frequency. Then, the optimal damping ratio of the ER damper and the appropriate voltage could be obtained. The experimental results indicate that the proposed feed forward control method is more effective in vibration isolation in comparison with the passive optimal system.

1. Introduction

In recent years, great attention has been focused on the design of control techniques of the two-stage vibration isolation system. Three types of vibration control methods have been proposed and implemented successfully, namely, passive method, active method and semi-active method.

*Corresponding author. Tel: +86-21-62932850; fax: +86-21-62933724.
E-mail address: suntao@sjtu.edu.cn (T. Sun).

0022-460X/$ - see front matter © 2004 Elsevier Ltd. All rights reserved.
doi:10.1016/j.jsv.2003.12.048

The semi-active control method plays an increasingly important role because it is more agile than the passive method and cheaper than the active method. With the development of the eletro-rheological (ER) fluid, the ER damper was found to shorten the control time and increase the reliability of the whole control system dramatically.

Most control strategies for semi-active vibration isolation systems are developed based on optimal control algorithms. As an exception, the application of adaptive control methods such as model reference adaptive control and non-linear self-turning control was investigated by Sunwoo and Cheok [1,2]. Generally, these controllers can minimize a defined performance index but may not have good capability to adapt to significant changes of the excitation signal and system parameters. The fuzzy inference, which is one of the knowledge-based approaches, has been applied recently into the design of semi-active vibration isolation systems with better performance because it is easier to control the system without considering the nonlinearity and uncertainty. Lin and Lu [3] built a model following fuzzy controller for vehicle suspension systems. Yoshimura et al. [4] used the displacement and velocity of the sprung mass and unsprung mass as the inputs of the fuzzy controller, and damper force as the output, to control the system by 49 fuzzy rules. Choi et al. [5,6] designed a neuro-fuzzy controller to control the semi-active ER suspension system and took the velocity of the sprung mass and the rotation angular speed of the wheel as the inputs. The results showed that the controller and the ER damper were effective to the suspension system. All the methods mentioned above are feedback control and have proven to improve the system performance.

The floating raft isolation system used in the ship, which has been developed during the past 20 years, is a typical vibration isolation system. It is deemed as a kind of efficient equipment for vibration isolation and noise reduction by isolating the vibrations of the host and auxiliary machines effectively [7,8]. Floating raft isolation system mainly uses the damper to isolate the vibration excited by the motors and bumps on the floating raft. Thus, the characteristics of the damper are crucial to the vibration isolation effect of the floating raft system. Varying from the road signals to the vehicle suspension system, the excitation signals of the floating raft isolation system are produced by some machines fixed on it. Therefore, it could be forecasted by analyzing the signal in frequency domain to assure whether the excitation signals are stable or changed regularly when these machines work normally. If the features of the excitation signal's main frequency can be learned in advance with some signal-processing techniques, a simple and better control scheme would be found readily to control the vibration isolation system.

Based on this mechanism, a novel feed forward fuzzy logic control method was developed to solve the problem in the semi-active two-stage vibration isolation system. The inputs of the fuzzy controller are the characteristics of the signal's main frequency, which are obtained by analyzing the excitation signal of the system, and the effect coefficient of the main frequency is chosen to be the output. Then, the optimal damping ratio and the corresponding control voltage of the ER damper can be figured out and the best isolation effect of the system could be realized. It indicates that the proposed fuzzy control method is more effective in the vibration isolation system than in the passive system through the experimental result.

Section 2 demonstrates the structures and differences of two types of the two-stage vibration isolation systems. The structure and the behavior of the ER damper are briefly explained in Section 3. Section 4 presents the proposed fuzzy control method in detail. Section 5 discusses the

experimental study and shows the results obtained. The conclusion of the work that has been done is given in Section 6.

2. Semi-active two-stage vibration isolation system

As shown in Fig. 1, there are two types of two-stage vibration isolation system, namely, active vibration isolation and passive vibration isolation. The objective of the active vibration isolation system is to decrease the forces transmitted to the foundation. For example, the floating raft isolation system in the ship is used to decrease the forces produced by the motors in order to make the base of the ship stable. In the passive vibration isolation system, however, the vibrant object is

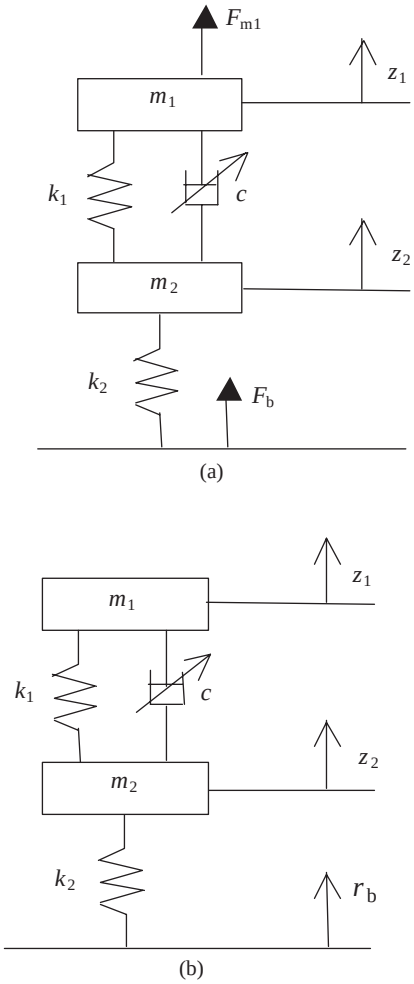

Fig. 1. The two-stage semi-active vibration isolation system: (a) active vibration isolation; (b) passive vibration isolation.

the base and the purpose of the control system is to keep the displacement of the upper object stable. Actually, two parameters have been defined to describe the capabilities of these two systems, the force transmission ratio T_f in active system and the displacement transmission ratio T_d in passive system. And it can be proven that these two parameters are naturally the same in one vibration isolation system.

Fig. 1 shows the structure of two dof vibration isolation systems modeled by the linear springs k_1 and k_2, the ER damper c that can be changed with the voltage applied, the sprung mass m_1 and the unsprung mass m_2. The displacements of the sprung mass and unsprung mass are presented by z_1 and z_2, respectively. Fig. 1(a) illustrates the active vibration isolation system and its equation of motion is

$$\begin{aligned} m_1\ddot{z}_1 &= -k_1(z_1 - z_2) - c(\dot{z}_1 - \dot{z}_2) + F_{m1}, \\ m_2\ddot{z}_2 &= k_1(z_1 - z_2) + c(\dot{z}_1 - \dot{z}_2) - k_2 z_2, \end{aligned} \tag{1}$$

where F_{m1} is the force produced by the sprung mass m_1 and F_b is the force transferred to the base. From Fig 1(a) it can be learned that

$$F_b = k_2 z_2. \tag{2}$$

Applying Laplace transform to Eq. (1),

$$\begin{aligned} (m_1 s^2 + cs + k_1)z_1(s) - (cs + k_1)z_2(s) &= F_{m1}(s), \\ (m_2 s^2 + cs + k_1 + k_2)z_2(s) - (cs + k_1)z_1(s) &= 0. \end{aligned} \tag{3}$$

Thus, the force transmission ratio $T_f(s)$ could be written as

$$T_f(s) = \frac{F_b(s)}{F_{m1}(s)} = \frac{k_2 cs + k_1 k_2}{m_1 m_2 s^4 + (m_1 + m_2)cs^3 + (m_1 k_1 + m_1 k_2 + m_2 k_1)s^2 + k_2 cs + k_1 k_2}. \tag{4}$$

Fig. 1(b) shows the passive vibration isolation system, where r_b is the displacement of the base. The system dynamics is described as

$$\begin{aligned} m_1\ddot{z}_1 &= -k_1(z_1 - z_2) - c(\dot{z}_1 - \dot{z}_2), \\ m_2\ddot{z}_2 &= k_1(z_1 - z_2) + c(\dot{z}_1 - \dot{z}_2) - k_2(z_2 - r_b) \end{aligned} \tag{5}$$

and its Laplace equation is

$$\begin{aligned} (m_1 s^2 + cs + k_1)z_1(s) - (cs + k_1)z_2(s) &= 0, \\ (m_2 s^2 + cs + k_1 + k_2)z_2(s) - (cs + k_1)z_1(s) &= k_2 r_b(s). \end{aligned} \tag{6}$$

The displacement transmission ratio $T_d(s)$ can be expressed as

$$T_d(s) = \frac{z_1(s)}{r_b(s)} = \frac{k_2 cs + k_1 k_2}{m_1 m_2 s^4 + (m_1 + m_2)cs^3 + (m_1 k_1 + m_1 k_2 + m_2 k_1)s^2 + k_2 cs + k_1 k_2}. \tag{7}$$

From Eqs. (4) and (7), we can see that the force transmission ratio $T_f(s)$ and the displacement transmission ration $T_d(s)$ are equal. In order to use the instruments and the test-bed in the laboratory, the passive vibration isolation system shown in Fig. 1(b) is analyzed here.

From Eq. (7), we can get the frequency response of sprung mass as shown in Fig. 2. It shows that there are two natural frequencies, the first-order and the second-order natural frequencies.

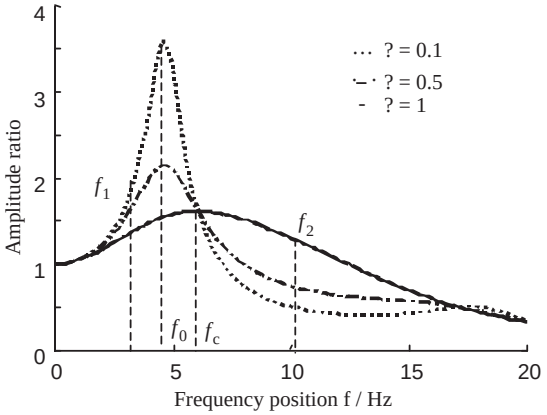

Fig. 2. The transmission ratio for various amounts of damping ratio.

Here, only the first-order frequency f_0 is considered because in most cases the vibration isolation system operates in low-frequency band rather than high-frequency band. The intercross frequency f_c is between the first-order and second-order natural frequencies. For an excitation signal with a single main frequency, we can easily choose the best damping ratio ξ_{OPT} to achieve the best isolation effect as shown in Fig. 2. When the main frequency is lower than f_c, we can use the maximal damping ratio ξ_{MAX} as ξ_{OPT}, and the minimal damping ratio ξ_{MIN} is applied when the main frequency is higher than f_c. However, for a complex input signal, we cannot use the above method to achieve best control effects because the signal has different main frequencies with different amplitudes. A best damping ratio ξ_{OPT} cannot be found readily in that some frequencies are lower than f_c, while others are higher with different amplitudes as shown in Fig. 2. In fact, many motors and bumps work together when the ship sails and the excitation signal to the floating raft isolation system contains many main frequencies at the same time. In order to solve this problem, a fuzzy controller is developed to select the best damping ratio ξ_{OPT} according to the features of the complex signal's main frequencies.

3. Properties of ER damper

The schematic diagram of the bypass ER damper used in this study is shown in Fig. 3. The damper consists of a hydraulic cylinder, which is divided into two working chambers by a piston. The bypass, fitted to the side of the hydraulic cylinder, comprises two concentric tubular electrodes and an annulus through which the ER fluids flow. The positive voltage produced by a high voltage supply unit is applied to the inner electrode, while the negative voltage is connected to the outer electrode. In the absence of electric fields, the ER damper produces the damping force only by the fluid-flowing resistance. However, if a certain level of the electric voltage is supplied to the ER damper, additional damping force due to the yield stress of the ER fluid would be produced. This damping force of the ER damper can be continuously tuned by changing the voltage applied to the damper.

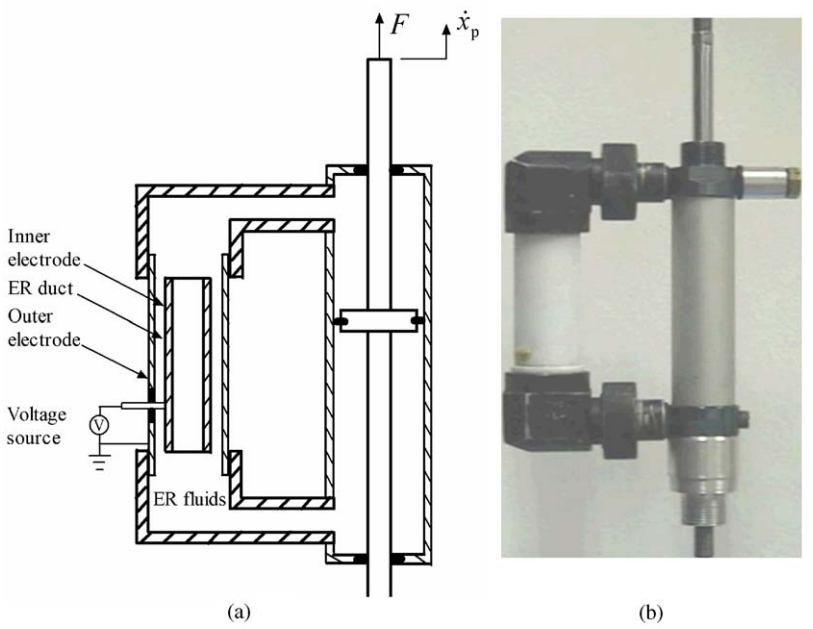

Fig. 3. The proposed ER damper: (a) schematic configuration; (b) photograph.

Based on the Bingham constitutive model of ER fluids [9–11], which is sufficiently accurate for design calculation although it does not capture details of the deformation behavior of an actual damper, the approximation of the damping force in the bypass damper is obtained as follows:

$$F = c_1 \dot{x}_p + F_{\mathrm{ER}} \operatorname{sgn}(\dot{x}_p), \tag{8}$$

where

$$F_{\mathrm{ER}} = \alpha_0 + \alpha_1 U + \alpha_2 U^2, \tag{9}$$

where c_1 is the viscous damping coefficient without applying voltage, which is determined by the plastic viscosity of ER fluids and the geometry of the manufactured damper, F_{ER} is the controllable damping force generated by the applied voltage, α_0, α_1 and α_3 are the intrinsic parameters of the ER damper and can be experimentally determined; U is the voltage; $\dot{x}_{\mathrm{P}}$ is the velocity of piston motion; and sgn( ) is a signum function.

Fig. 4 reports the measured damping force with respect to the piston velocity at various voltages. It is obtained by calculating the maximum damping force at each velocity. The piston velocity increases from 15 to 100 mm/s gradually, while the excitation amplitude is maintained to be constant, e.g. 60 mm. Such a plot is frequently employed to evaluate the level of damping performance in damper manufacturing industry. For the proposed damper, the damping force increased with the applied voltage, as expected. For instance, the damping force increases up to 217 N at a piston velocity of 100 mm/s and voltage of 5 kV. This figure agrees fairly well with the presented damping model given by Eq. (8).

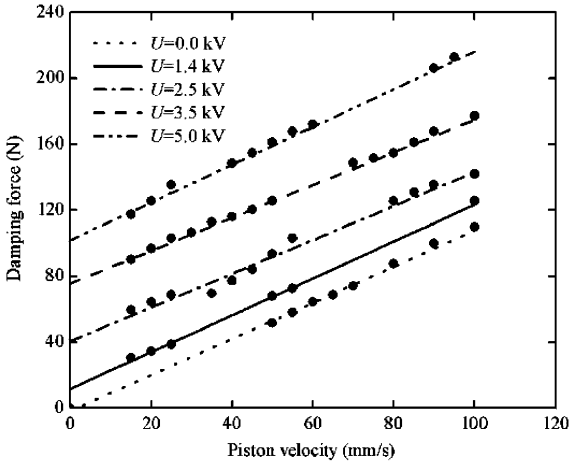

Fig. 4. Damping force versus piston velocity at various voltages.

For the two-stage vibration isolation system shown in Fig. 1(a), the following relations can be obtained:

$$F = c\dot{x}_p \tag{10}$$

and

$$c = 2\xi\sqrt{m_1 k_1}, \tag{11}$$

where c, m_1 and k_1 are the same parameters show in Eq. (1).

Replacing F and F_{ER} in Eq. (8) with Eqs. (9) and (10), we get

$$2\xi\sqrt{m_1 k_1}\dot{x}_p = c_1\dot{x}_p + (\alpha_0 + \alpha_1 U + \alpha_2 U^2)\,\mathrm{sgn}(\dot{x}_p). \tag{12}$$

In Eq. (12), the relationship between the damping ratio ξ and the control voltage U of the ER damper is obtained. When the optimal damping ratio ξ_{OPT} is obtained by the fuzzy controller, the ER damper's control voltage can be calculated.

4. Fuzzy control system

The structure of the control system is demonstrated in Fig. 5. It mainly consists of three parts: the identification of signal main frequency, fuzzy controller and the output of control voltage. When the control system runs, the first part will find the characteristics of the signal's main frequency and send them to the fuzzy controller. Then, the fuzzy controller makes the decision according to the rules and selects the best effect coefficient of each main frequency. Finally, the third part will find the best damping ratio of the ER damper and transform it into the corresponding voltage that will then be applied to the ER damper.

4.1. Identification of excitation signal

The signals in engineering vary widely and it is difficult to classify them accurately. Here we just take into account those signals made by some motors or bumps in the ship or some machines. It could be divided into two classes from the point of frequency domain, the stationary signal and the non-stationary signal. There are two important parameters for describing the signal in frequency domain that could show its effect on the system. One is the signal's frequency position that indicates mainly in which frequency band the signal's energy is. The other is the main frequency's amplitude denoting the signal's magnitude. The stationary signal implies that the signal's characters, including the main frequency's position and amplitude, do not vary with time. The non-stationary signal here means that these characters of the signal change continually. For example, the sine or cosine signal with fixed frequency is the stationary signal, while the sweep-frequency signal is the non-stationary signal whose main frequency is changed by rule. As shown in Fig. 2, different main frequencies have various effects on the two-stage vibration isolation system. Consequently, how to distinguish the main frequency characters of the signal, especially the main frequency's position and amplitude, is very important to realize the control.

Fig. 6 shows the process of identifying the signal's frequency characters. Obviously, the signal is divided into two classes and each has different handling methods. The Short-time Fourier

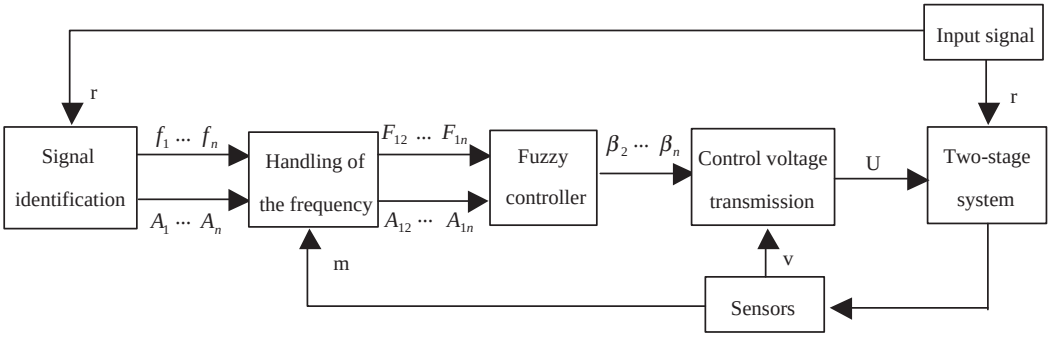

Fig. 5. The structure of the fuzzy control system.

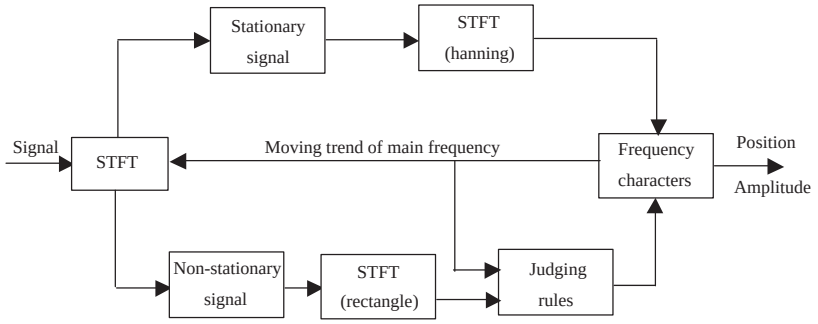

Fig. 6. Identification of the signal's main frequency.

Transform (STFT) algorithm processes the excitation signal at first. After that, the signal will be split into two classes according to the moving trend of its main frequency. The processing of these two types of signals is explained, respectively, in the following paragraphs.

4.1.1. Identification of stationary signal

The stationary signal's main frequency characters can be easily obtained after the STFT algorithm. It is obvious that the moving trend of the main frequency is fixed at the beginning of this process because the main frequency remains unchanged. Therefore, the stationary signal can be identified quickly, which means its characteristics, the main frequency's position and amplitude can be figured out through the STFT algorithm. The choosing of the window function is quite critical because it can enhance the identification precision of the STFT algorithm. It is learned from the simulation that the rectangle window function is not qualified enough here because it can cause the frequency leakage. Thus, the hanning window is employed to find the exact frequency characters of the stationary signal.

4.1.2. Identification of non-stationary signal

For the non-stationary signal, it is hard to find its main frequency characters due to the successively changing moving trend of the main frequency. In such a case, the result may be coarse if only the STFT algorithm is applied because the changing trend is more important for the non-stationary signal. For example, the main frequency is 4 Hz after the STFT algorithm in a moment, but before this moment the main frequency is 15 Hz and it becomes higher at a velocity of 3 Hz/s. Consequently, 4 Hz is not logical and it should be replaced by one frequency bigger than 15 Hz. In order to achieve the exact identification, the STFT algorithm and the moving trend of the main frequency are combined to complete the analyzing of the non-stationary signal. A similar problem also exists when choosing the window function for the STFT algorithm. The hanning window function prefers to cause the lag of the identification because it only weights the signal frequency in the middle of the window, while attenuating the others. This will lead to the mistiness of the main frequency and influence the accuracy of the identification. In this regard, the rectangle window was employed because it has a smaller central lobe. During the whole signal-identifying process, the rectangle window's width could be adjusted with the moving trend of the main frequency in order to acquire the proper frequency characteristics, the main frequency's position and amplitude.

4.2. Fuzzy controller

The main frequency's characteristics, including the positions and amplitudes, can be revealed through the signal identification. Here we define the amplitudes as $A_1, A_2, \ldots, A_n$ where $A_1 \geqslant A_2 \geqslant \cdots \geqslant A_n$. According to the effect of the main frequency on the isolation system, the following equations are built to find the optimal damping ratio of the ER damper:

$$Y(\xi) = A_1 G(f_1, \xi) + \sum_{2}^{n} \beta_{1i} A_i G(f_i, \xi), \quad i = 2, 3, \ldots, n, \tag{13}$$

$$G(f_i,\xi) = \mathrm{abs}\left(\frac{2k_2\xi\sqrt{m_1k_1}f_i + k_1k_2}{m_1m_2f_i^4 + 2(m_1+m_2)\xi\sqrt{m_1k_1}f_i^3 + (m_1k_1+m_1k_2+m_2k_1)f_i^2 + 2k_2\xi\sqrt{m_1k_1}f_i + k_1k_2}\right), \tag{14}$$

where $G(f_i,\xi)$ $(i=1,2,\ldots,n)$ is the modulus of the system transfer function at f_i and related to the damping ratio ξ; β_{1i} $(i=2,3,\ldots,n)$ is the weighting coefficient of every main frequency acquired by the fuzzy controller; $Y(\xi)$ is the displacement response curve of the sprung mass when the system is bestirred by different main frequencies simultaneously. The optimal damping ratio ξ_{OPT} could be acquired while Y in Eq. (13) is minimal.

4.2.1. Fuzzification of the input and output variable

Three coefficients, position coefficient F_{1i}, amplitude coefficient A_{1i} and effect coefficient β_i $(0<\beta_i<1)$, are defined here in order to describe the characters of the main frequency. F_{1i} and A_{1i} are used as the two input variables of the *ith* fuzzy controller and the effect coefficient β_i as the output variable.

4.2.1.1. Fuzzification of position coefficient F_{1i}. The form of coefficient F_{1i} is given by

$$F_{1i} = \begin{cases} |f_1 - f_0|/|f_i - f_0|, & f_i \neq f_0 \\ 5, & f_i = f_0 \end{cases} \quad i = 2,3,...,n, \tag{15}$$

where f_0 is the first-order natural frequency; f_1 is the main frequency whose amplitude is the biggest and f_i $(i=2,3,\ldots,n)$ stands for the other main frequencies.

It is obvious from Eq. (15) that F_{1i} indicates the relative position between main frequency f_1 and f_i. F_{1i} decreases when f_1 is near the resonant frequency f_0 and its influence to the system is more significant than f_i. The universe of discourse for F_{1i} is taken as [0 5] according to its definition (let $F_{1i}=5$, if $F_{1i}>5$). When F_{1i} is near 1, that is to say, the main frequency f_1 and f_i have similar effects on the isolation system. The universe of discourse for the input variables is divided into five sections by using the following linguistic variables, i.e. very small (VS), small (S), middle (M), big (B), and very big (VB). The membership function curve is a little denser in [0 1] than in [1 5] to realize accurate control because the meaning of the position coefficient F_{1i} that is bigger than 1 is the opposite of that when it is smaller than 1.

4.2.1.2. Fuzzification of amplitude coefficient A_{1i}. A_{1i} is given by

$$A_{1i} = A_1/A_i, \quad i = 2,3,\ldots,n \tag{16}$$

From Eq. (16), we can find that A_{1i} gives the ratio of A_1 over A_i. A_{1i} is bigger than 1 because A_1 is the biggest amplitude of all the main frequencies. Generally speaking, the effect of main frequency f_i on the system is smaller when the amplitude coefficient A_{1i} is bigger. We consider that main frequency (f_i)'s effect is extremely small when the amplitude coefficient A_{1i} is bigger than 5. Therefore, the universe of discourse for input A_{1i} is chosen as [1 5] (let $A_{1i}=5$, if $A_{1i}>5$) and its linguistic variables and the shape of membership function curve are similar with F_{1i}.

4.2.1.3. Fuzzification of effect coefficient β_i. The output variable of the fuzzy controller, effect coefficient β_i ($0<\beta_i<1$), is the weightiness of the main frequency f_i when the system is bestirred by the two main frequencies f_1 and f_i together. It is clear that the weightiness of main frequency f_i is bigger if the effect coefficient β_i is bigger. The universe of discourse for β_i is [0 1] and its linguistic variables are taken as small (S), middle (M) and big (B). Here three linguistic variables are used in order to keep the continuity and stability of the control voltage.

Fig. 7 illustrates the membership functions of the input and output variables. Triangular membership functions are chosen because they are very basic and have been widely used.

4.2.2. Fuzzy control rules

The empirical knowledge to construct the fuzzy control rules is presented as follows:

(1) If F_{1i} is big or very big, and A_{1i} is small or very small, then β_i is big.
In this case, F_{1i} is big or very big, that is to say, f_1 is farther away from the first-order natural frequency f_0 than main frequency f_i. Hence, f_i's effect on the whole vibration isolation system is more significant than f_1 in terms of the position coefficient F_{1i}. At the same time, A_{1i} is small or very small, that means the amplitudes of both the two main frequencies, f_1 and f_i, are similar. In this case, we think f_i's effect on the system is considered to be bigger than f_1 and it is reasonable to focus on f_i. What's more, the effect coefficient β_i is big herein. For example, there are two excitation signals that are both sines at the same time. The main frequency f_1 is 2 Hz with amplitude 1 cm, and f_2 is 5 Hz with amplitude. The first-order natural frequency f_0 is 4.5 Hz. The position and amplitude coefficients can be acquired with the values of 5 and 1.

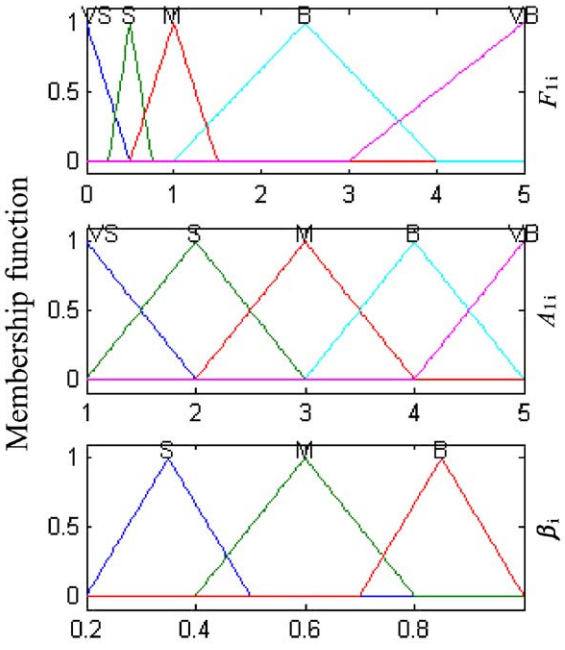

Fig. 7. Membership function of the input and output variables.

Apparently, F_{1i} is very big and A_{1i} very small, and the effect coefficient β_i is taken as 0.9 in this case in order to give more attention to the main frequency f_2.

(2) If F_{1i} is small or very small, and A_{1i} is big or very big, then β_i is small.
This rule is opposite to the first rule and can be deduced easily.

(3) If F_{1i} and A_{1i} are both big or very big, then β_i is middle.
This rule means that f_i should be considered more from the point of position coefficient F_{1i} and f_1 is a little important to the system in terms of amplitude coefficient A_{1i}. So a compromise between F_{1i} and A_{1i} is made and the effect coefficient β_i is middle.

(4) If F_{1i} and A_{1i} are both small and very small, then β_i is middle.

This case is opposite to rule 3.

Based on the above empirical knowledge, 25 various fuzzy control rules were derived and are shown in Table 1. They can be described by the linguistic form:

$$R_j : \text{If } F_{1i} \text{ is } C_j \text{ and } A_{1i} \text{ is } D_j \text{ then } \beta_i \text{ is } E_j,\ j = 1, 2, ..., 25,$$

where F_{1i}, and β_i are, respectively, the input and output variables; C_j, D_j, and E_j are the as fuzzy sets whose membership functions are respectively shown in Fig. 7.

4.2.3. *Defuzzification of the output*

The defuzzification procedure employed is the centroid of area method. This method is sufficient for the controller and is one of the most popular means available.

$$\beta_i = \sum_{m=1}^{N} x_m \mu_{\beta_i^0}(x_m) \Big/ \sum_{m=1}^{N} \mu_{\beta_i^0}(x_m), \quad i = 2, 3, \ldots, n, \tag{17}$$

where β_i^0 is the fuzzy set of the output; x_m is the element in the output variable's universe of discourse; $\mu_{\beta_i^0}(x_m)$ is the membership function of x_m and N is the number of the fuzzy set which x_m belongs to.

From the discussion mentioned above, we learn that the effect coefficient β_i denotes the effect of main frequency f_i, and, apparently, the effect of the main frequency f_1 can be defined as $1 - \beta_i$. In order to simplify the formula, the weighting coefficient β_{1i} in Eq. (13) can be figured out by the following equation when the effect coefficient of main frequency f_1 is taken as 1:

$$\beta_{1i} = \beta_i/(1 - \beta_i), \quad i = 2, 3, \ldots, n. \tag{18}$$

Table 1
Fuzzy control rules of fuzzy controller

β_i		F_{1i}				
		VS	S	M	B	VB
A_{1i}	VS	M	M	B	B	B
	S	S	M	B	B	B
	M	S	S	M	M	B
	B	S	S	M	M	B
	VB	S	S	S	M	B

So far, all the parameters in Eq. (13) have been obtained and the optimal damping ratio ξ_{OPT} can be figured out accordingly.

4.3. Output of the voltage

The optimal damping ratio ξ_{OPT} figured out from Eq. (13) must be transferred into the voltage of the ER damper. From Eq. (12), the appropriate voltage can be determined. The relative velocity of the damper piston, $\dot{x}_P$, can be measured by the sensors. One important point that should be noticed is that the ER damper has a permitted voltage U_{MAX} in order to operate safely. If the transferred voltage is higher than U_{MAX}, U_{MAX} would be used to replace it in order to protect the ER damper from damage.

5. Experiment and results

For the two-stage vibration isolation system given in Section 2, the parameter values used for the experiment are given as: $m_1 = 60\,\text{kg}$, $m_2 = 16\,\text{kg}$, $k_1 = 33\,\text{kN/m}$, $k_2 = 185\,\text{kN/m}$, $U_{MAX} = 4\,\text{kV}$. From these parameters, we can get the formant frequency and the intercross frequency of the real system: $f_0 = 3\,\text{Hz}$, $f_c = 5\,\text{Hz}$. The experiment was carried out in the State Key Laboratory of Vibration, Shock and Noise. The setup of the experimental equipment is displayed in Fig. 8.

Fig. 9(a) illustrates the acceleration of the excitation signal. The signal is composed of two sine waves that can be denoted as follows:

$$\begin{aligned} &4\sin(2\pi 3t) + \sin(2\pi 7t), \quad 0-1s,\\ &\sin(2\pi 3t) + 4\sin(2\pi 7t), \quad 1-2s,\\ &4\sin(2\pi 2t) + \sin(2\pi 7t), \quad 2-3s. \end{aligned} \tag{19}$$

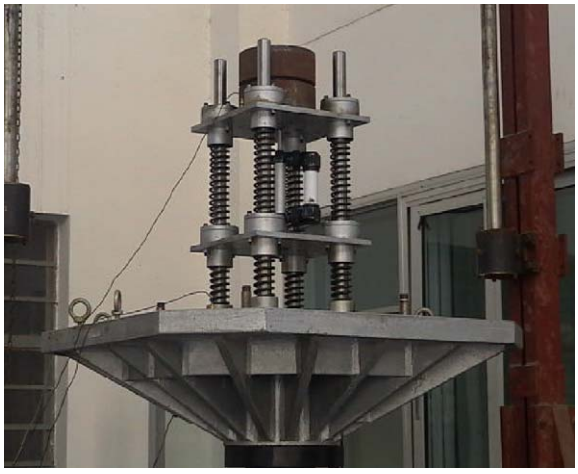

Fig. 8. Photograph of the experimental apparatus.

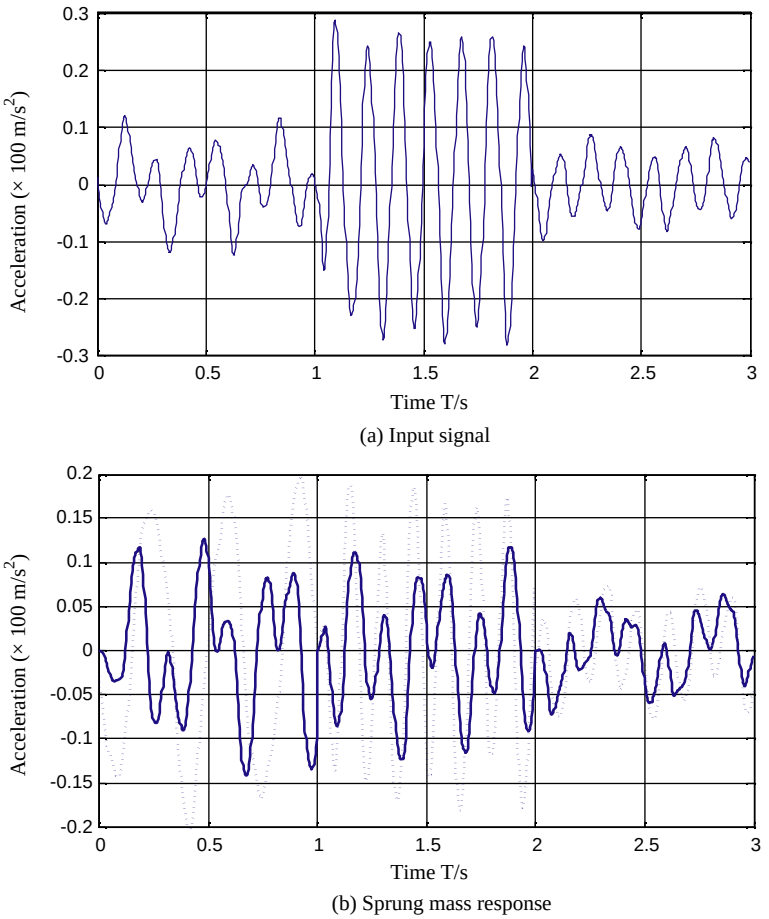

Fig. 9. Acceleration of the excitation signal and the sprung mass.

Fig. 9(b) shows the acceleration of the sprung mass. The dotted line denotes the optimal passive system with the damping coefficient $\xi_P = 0.7$, while the real line denotes the semi-active fuzzy control system. It was learned that the control effect of the semi-active fuzzy control system is better than the optimal passive system all the time, by a decrease of 15–50% through the fuzzy control. The reason for the better performance is that fuzzy control system can get the optimal damping ratio ξ_{OPT} by analyzing the frequency of the signal in three different sections, while the optimal passive system employs the same damping ratio $\xi_P = 0.7$ all the time. The amplitude of the main frequency 3 Hz is four times of that of the main frequency 7 Hz before the 1st second. The effect of main frequency 3 Hz on the whole system is very important because its amplitude is bigger and its position is nearer to the formant frequency f_0. Hence, the fuzzy control system paid more attention to the main frequency 3 Hz and adopted the optimal damping ratio $\xi_{OPT} = 1$ with the corresponding voltage as 4 kV. The situation was reversed during the 1st and 2nd second and the main frequency is more important to the system. The fuzzy control system uses $\xi_{OPT} = 0.1$ and $U = 0$ kV. During the last time section, one of the main frequencies changed from 3 to 2 Hz, where

the amplitude was four times that at the main frequency 7 Hz. Although its amplitude is big, it is a little far away from the formant frequency. Therefore, its effect on the system was not very dramatic. The fuzzy control system used $\xi_{OPT} = 0.3$ and U = 1 kV after considering the two main frequencies' positions and amplitudes.

Fig. 10 shows the displacement of the sprung mass. The excitation signal is the superposition of two sine sweeping signals. One changed from 0 to 10 Hz, while the other from 10 to 0 Hz during 30 s. That means, the system was excited by two main frequencies at the same time and these main frequencies varied with the time. Figs. 10(a) and 10(b) illustrate the displacements of the sprung mass of the optimal passive system, and the semi-active fuzzy control system respectively. It is clear that the vibration isolation effect is better in Fig. 10(b) than that in Fig. 10(a) because fuzzy control system can provide the optimal damping ratio and voltage in every sample time. The sprung mass' frequency response is denoted in Fig. 11. It was found that the amplitude ratio of the

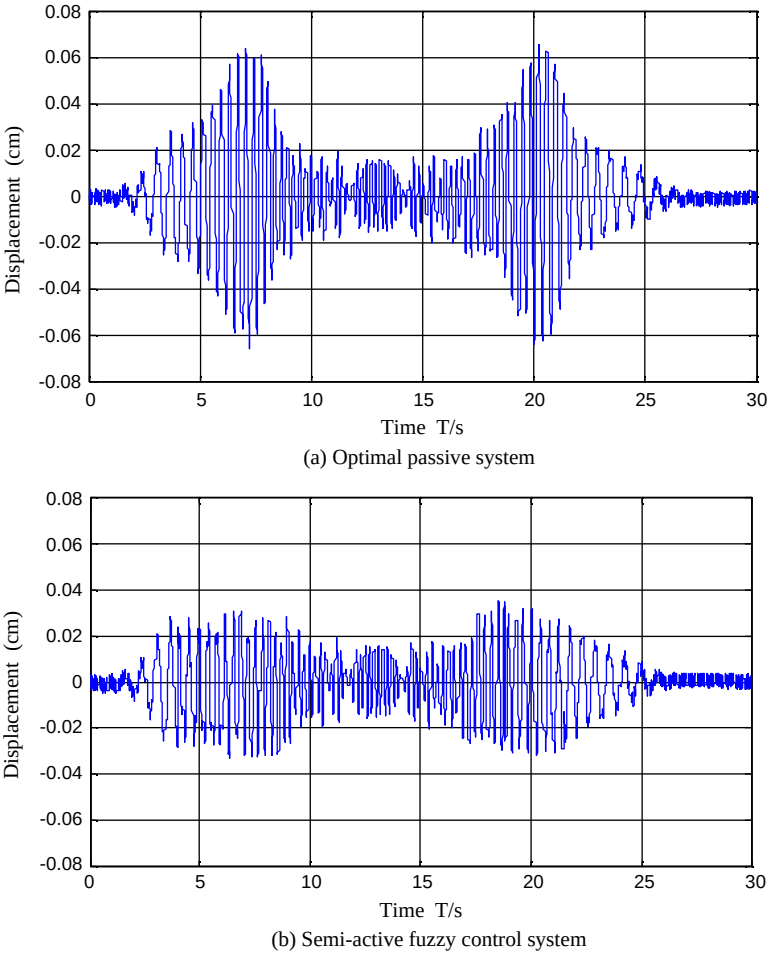

Fig. 10. Displacement of sprung mass under the chirp excitation system.

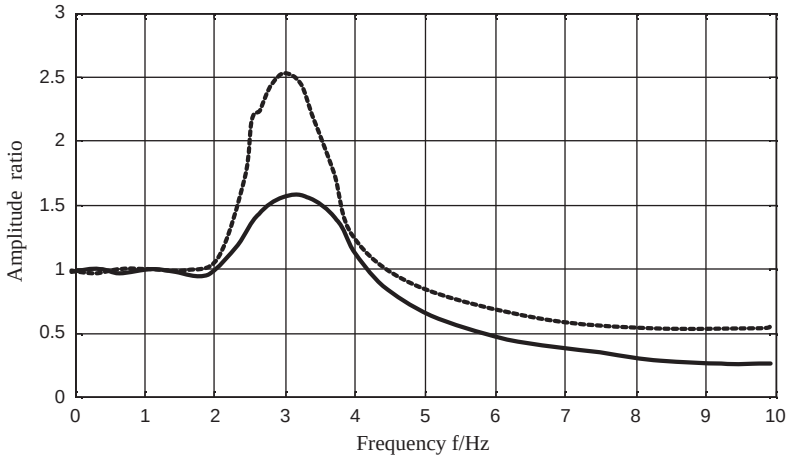

Fig. 11. Transmission ratio of the optimal passive system and the semi-active fuzzy control system under chirp excitation signal.

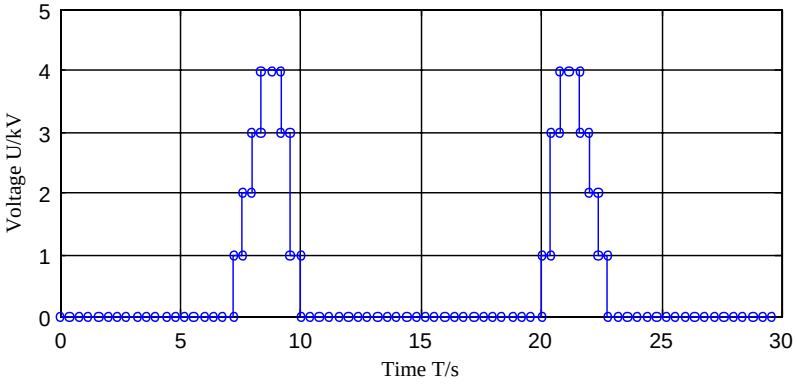

Fig. 12. Voltage of the damper under the chirp excitation system.

fuzzy control system is lower than that of the optimal passive system in the whole frequency band. The voltage of the damper is shown in Fig. 12.

6. Conclusions

In summary, this paper proposed a new feed forward fuzzy control method for the semi-active vibration isolation system with an ER damper. It is simpler and rapider than the feedback control methods because the feedback information does not need to be used in it. The experimental results indicate that the proposed semi-active control method is better in enhancing the performance of the vibration isolation system in comparison with the passive control one. Three merits of the control system are concluded as follows:

(1) It brings forward a method in frequency domain to identify the characters of the excitation signal's main frequency as well as the main frequency's position and amplitude. In order to identify these characters more accurately, various methods are employed according to stationary and non-stationary signals, respectively.
(2) It uses the fuzzy controller to find the weightiness of every main frequency. The rules of the fuzzy controller are made experientially and can be adjusted according to the change in the system parameters. Therefore, the vibration isolation system is able to find the best damping ratio and voltage of the ER damper.
(3) The semi-active vibration isolation system is combined with the ER damper. Using the character of the ER fluids, the control effect of the whole system becomes faster and more reliable.

References

[1] M. Sunwoo, K.C. Cheok, An application of explicit self-tuning controller to vehicle active suspension system, *Proceedings of the 29th IEEE Conference on Decision and Control*, Vol. 4, 1990, pp. 2251–2265.
[2] M. Sunwoo, K.C. Cheok, An application of model reference adaptive control to active suspension system, *Proceedings of the 1990 American Control Conference*, Vol. 2, 1990, pp. 1340–1356.
[3] Y.J. Lin, Y.Q. Lu, Fuzzy logic control of vehicle suspension systems, *International Journal of Vehicle Design* 14 (5) (1993) 457–470.
[4] T. Yoshimura, H. Kubota, K. Takei, M. Kurimoto, J. Hino, Construction of an active suspension system of a quarter car model using fuzzy reasoning based on single input rule modules, *International Journal of Vehicle Design* 23 (3/4) (2000) 297–306.
[5] S.B. Choi, Y.T. Choi, E.G. Chang, S.J. Han, C.S. Kim, Control characteristic of a continuously variable damper, *Mechatronics* 8 (1998) 143–1611.
[6] S.B. Choi, M.S. Suh, D.W. Park, M.J. Shin. Neuro-fuzzy control of a tracked vehicle featuring semi-active electro-rheological suspension units, *Journal of Vehicle System Dynamics* 35 (3) (2001) 141–162.
[7] T.Y. Li, X.M. Zhang, Y.T. Zuo, M.B. Xu, Structural power flow analysis for a floating raft isolation system consisting of constrained damper beams, *Journal of Sound and Vibration* 202 (1) (1997) 47–54.
[8] Z.Q. Qu, W.J. Chang, Dynamic condensation method for viscously damper vibration systems in engineering, *Engineering Structures* 23 (2000) 1426–1432.
[9] H.P. Gavin, R.D. Hanson, F.E. Filisko, Electrorheological dampers—part I: analysis and design, *Journal of Applied Mechanics* 63 (1996) 669–675.
[10] H.P. Gavin, R.D. Hanson, F.E. Filisko, Electrorheological dampers—part II: testing and modeling, *Journal of Applied Mechanics* 63 (1996) 669–675.
[11] L. Jason, M.W. Norman, Analysis and testing of electrorheological bypass dampers, *Journal of Intelligent Material Systems and Structures* 10 (1999) 363–376.